Earthquake Engineering, Tenth World Conference © 1992 Balkema, Rotterdam. ISBN 90 5410 060 5

Evaluation of ultimate capacity for seismic isolation layer considering randomness of rubber bearing

Kazuta Hirata
Central Research Institute of Electric Power Industry, Japan
Takahiro Somaki, Hidemasa Tomura & Kenji Shirahama
Nuclear Facilities Division, Obayashi Corporation, Japan

ABSTRACT: This paper describes the results of reliability analyses for the seismic isolation layer based on static and dynamic Monte Carlo Simulations, considering rupture phenomena of seismic isolators, to investigate the safety of the seismic isolation system (the base isolation system) for FBR (Fast Breeder Reactor) building. Parameters used in the analyses are the variation in the rupture strength of the seismic isolator (COV: the coefficient of variation), the figure of the FBR building (H: the height of the center of gravity), and the input peak ground acceleration. Based on the analytical results, the ultimate capacity of the entire seismic isolation system and the influence on the response of the superstructure by the rupture phenomena are evaluated, and the failure propability (fragilty curve) of the seismic isolation layer is estimated.

1 INTRODUCTION

It is required to reduce seismic load by introducing the seismic isolation system in the FBR building, in which equipments are subject to thermal stress. Recently, many studies on the application of the seismic isolation system have been conducted, which has been adopted in some general buildings.

Rupture strength of the laminated rubber bearings (isolators), of which the seismic isolation layer is composed, varies due to materials and the manufactering condition. As the high seismic reliability is required to FBR system, it is very essential to grasp the ultimate capacity and behavior of the seismic isolation layer considering the randomness of the seismic isolation devices, and to evaluate the stability of the layer. However, studies on the reliability of the seismic isolation system focused on the rupture phenomena have not been conducted yet.

Here, the reliability analyses based on static and dynamic Monte Carlo Simulations (S-MCS and D-MCS, respectively), considering the variation in the rupture strength of the seismic isolators, are conducted to investigate the subjects mentioned above. Further, the relation between partial rupture phenomena and whole rupture is qualitatively evaluated.

2 METHOD OF ANALYSIS

2.1 Analytical Model

As shown in Fig.1, the FBR building supported by the seismic isolation system is considered. Since the horizontal stiffness of the isolation layer is much smaller than that of the superstructure, the analytical model can be simplified as a one-lumped mass model with the mass located at the center of the gravity as shown in Fig.2. The weight of the superstructure (about 136,000 tons) is concentrated at the height (H) of the center of the gravity. The seismic isolation devices (lead rubber bearings) with the design vertical load of 500 tons (25 kg/cm^2) are installed at equal intervals in 16 rows by 17 rows, and in total 272 units under the upper base mat. The mass is connected to each device bya rigid beam and the upper base mat.

2.2 Mechanical properties

Mechanical properties for the seismic isolation devices are represented in Fig.3. Horizontal hysteresis rule for the isolator (Fig.3(a)) is modeled with 3 straight lines(α,β,γ- lines). Vertical hysteresis rule for the isolator(Fig.3(b))is modeled with 2 straight lines in the tensile region and a single straight line in the compressive region. After rupture, the isolator is assumed to bear only compressive load with one half of the initial compressive stiffness. Horizontal hysteresis rule for the lead damper (Fig.3(c)) is a complete elasto-plastic model. With the total stiffness of the isolators and the dampers, the natural period of the isolated building in the horizontal direction is 1 second, and with the total stiffness of only isolators the natural period is 2 seconds.

2.3 Criteria of rupture

As shown in Fig.4, rupture criteria of the isolator is given by rupture surface with shear strain and vertical stress[1]. In case the isolation device is subjected to only tensile force, the mean tensile rupture strength is 50 kg/cm². And in case only shear force is loaded, the mean shear rupture strain is 450%. If vertical and horizontal forces are applied simultaneously, the mean rupture criteria is defined by the straight line connected above 2 points.

As for the variation of the rupture strength, Gaussian distribution is assumed. The rupture surface of each isolator varies between dotted lines shown in Fig.4. The dotted lines denote lower (0.5 times mean) and upper (1.5 times mean) limit of the rupture surface.

2.4 Input ground motion

Time history of the artificial input ground motion (original wave) with relatively long period content is shown in Fig.5.

The maximum acceleration of the original wave is approximately 330gal. The time duration of the wave used for analysis is 30 seconds including the preliminary tremors.

2.5 Analytical parameters

As shown in Table 1, analytical parameters for S-MCS are the figure of the building (H: 5.0m - 22.5m, the height of the center of gravity) and the variation in the rupture strength of the isolator (COV: 0% - 40%, the coefficient of variation), and those for D-MCS are COV (0% - 20%) and the maximum input acceleration (1,050gal - 1,175gal). Herein, the COV of 20% and the H of 22.5 meters are set as the standard case.

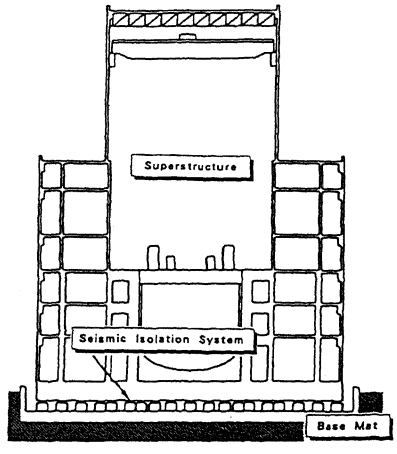

Fig. 1 FBR building supported by the seismic isolation system.

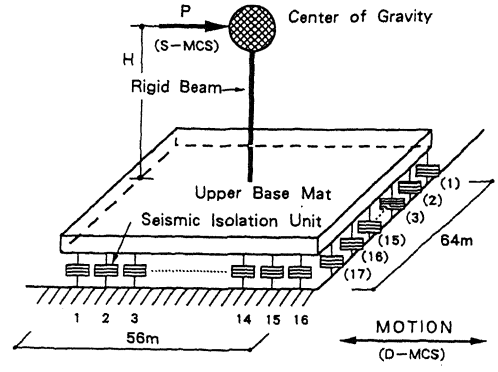

Fig. 2 Analytical model.

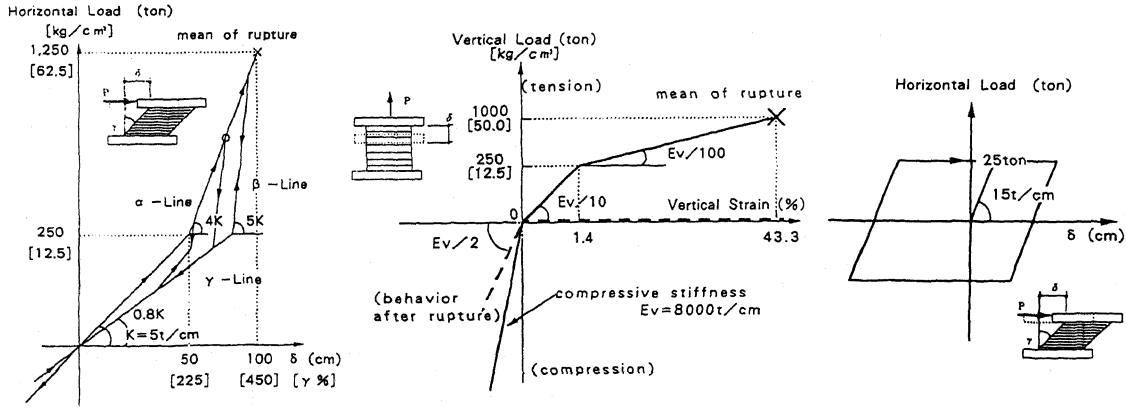

(a) Horizontal hysteresis rule for the isolator. (b) Vertiacl hysteresis rule for the isolator. (c) Horizontal hysteresis rule for the lead damper.

Fig. 3 Relationship between load and displacement for the seismic isolation device.

As the input acceleration level is gradually increased, the ratio of the ruptured isolators increases from 10% to over 50% at the end of the analysis. These analyses are performed 100 times in each case for S-MCS, and 50 times for D-MCS.

2.6 Procedure

The non-linear static analysis in which by the monotonous loading is applied at the mass point is carried out for S-MCS, and the non-linear dynamic response analysis is done for D-MCS. The input ground motion (Fig.5) is applied in one direction to the analytical model (Fig.2). The incremental time is 0.002 second for the dynamic response analysis.

The unbalanced force generated by the change of the stiffness is released as an external force at the next time step. The force released by the rupture phenomena of the isolator is converged within the current time step.

Torsional response of the base mat by the unsymmetric rupture of the isolators is not considered.

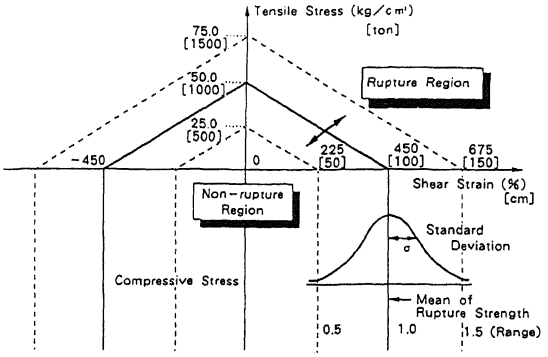

Fig. 4 Criteria of rupture.

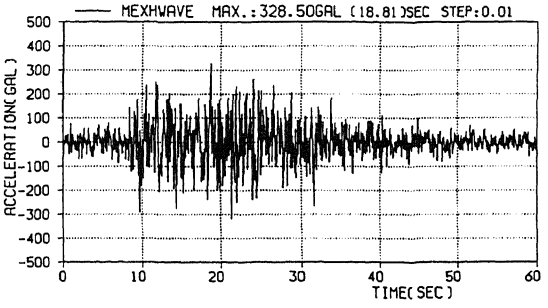

Fig. 5 Input ground motion (artificial earthquake).

Table 1 List of calculated cases

	Static - MCS					Dynamic - MCS			
Case No.	H* (m)	COV** (%)	Acceleration (gal)	N***	Case No.	H* (m)	COV** (%)	Acceleration (gal)	N***
S1	22.5	20	—	100	D1	22.5	20	1,050	50
S2	20.5	20	—	100	D2	22.5	20	1,075	50
S3	17.5	20	—	100	D3	22.5	20	1,100	50
S4	15.0	20	—	100	D4	22.5	20	1,125	50
S5	12.5	20	—	100	D5	22.5	20	1,150	50
S6	10.0	20	—	100	D6	22.5	20	1,175	50
S7	7.5	20	—	100	D7	22.5	0	1,125	1
S8	5.0	20	—	100	D8	22.5	0	1,150	1
S9	22.5	0	—	1	D9	22.5	0	1,175	1
S10	22.5	10	—	100					
S11	22.5	30	—	100					
S12	22.5	40	—	100					

* height of the center of gravity(see Fig.2)
** coefficient of variation in the rupture strength of the isolators(= σ/m, see Fig.4)
*** number of simulations in MCS

3 CALCULATED RESULTS

Fig.6 shows examples of the relationship between the shear force and the horizontal displacement (P-δ relationship) for the seismic isolation layer. P-δ relationship differs between the results by S-MCS and D-MCS, because ruptured isolators increase during the reversal loadings in D-MCS.

Based on the results of S-MCS, the maximum shear strength(Pmax) and the horizontal displacement at Pmax of the seismic isolation layer are shown in Fig.7. Pmax becomes smaller as COV in the rupture strength of the isolator and the center of the gravity height H become respectively greater and higher, and the displacement at Pmax becomes smaller with increasing H, but becomes larger as the COV is greater.

Fig.8 and Fig.9 show the comparison between the case (D6, No.1; 1,175gal) considering the rupture and the one without considering the rupture, regarding the time history of the response acceleration at the

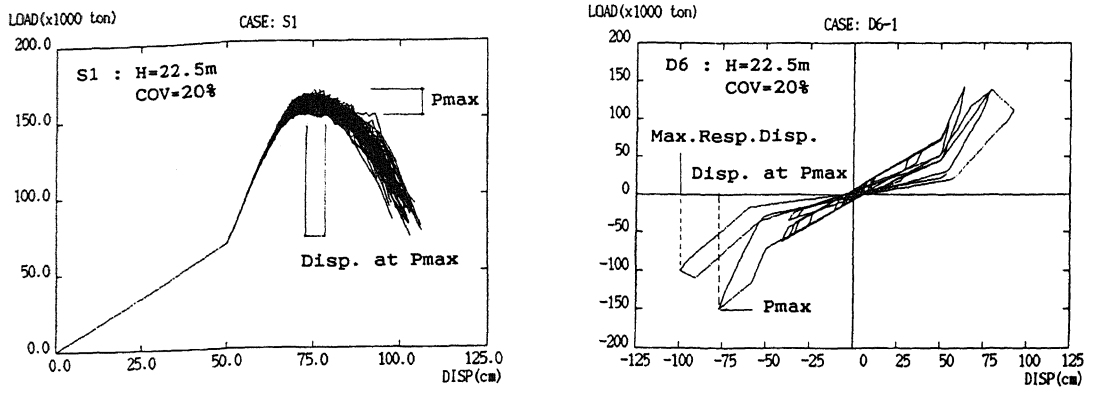

(a) S-MCS (S1, No.1 - 100).

(b) D-MCS (D6, No.1).

Fig. 6 Examples of relationship between the shear force and the horizontal displacement of the seismic isolation layer.

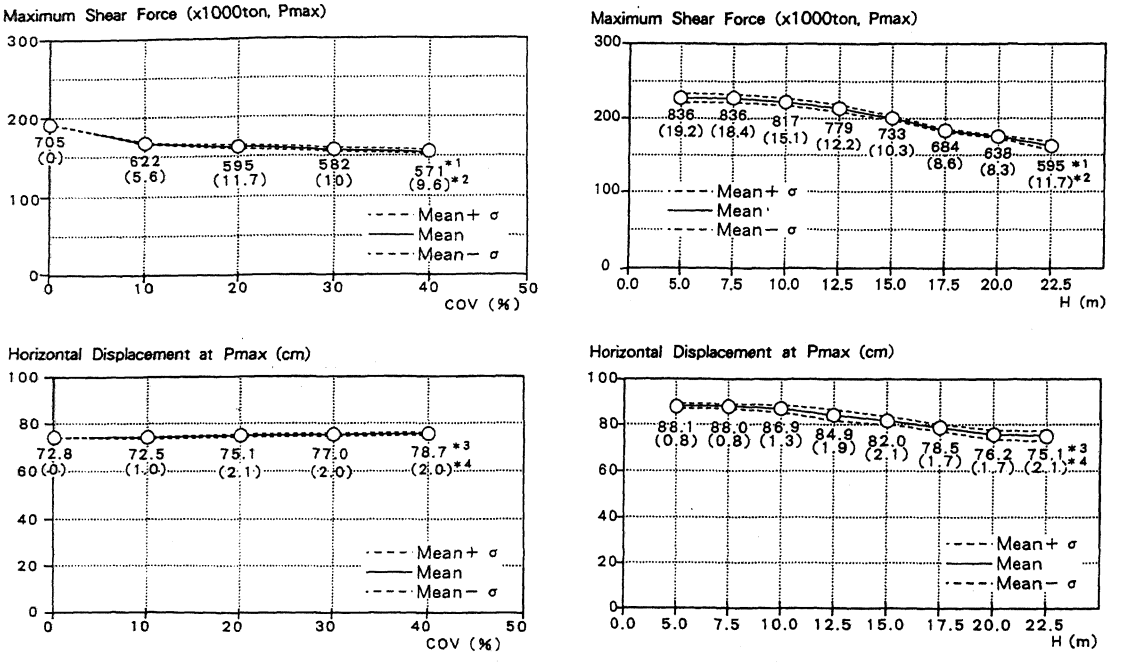

(a) Effect of the COV.

(b) Effect of the center of gravity height (H).

[Note] 1) *1 and *2 are the mean and the standard devition of the applied shear force per unit (= Pmax / 272 units), respectively.
2) *3 and *4 are the mean and the standard deviation of the horizontal displacement at Pmax, respectively.

Fig. 7 The maximum shear strength (Pmax) and the horizontal displacement at Pmax of the seismic isolation layer based on the results of S-MCS.

center of gravity and the floor response spectrum of acceleration. Fig.8 shows that there is some difference in two responses due to the rupture phenomena, especially after 25 seconds the period of the system elongates in the case where rupture of the isolators are taken into account. Fig.9 shows that the response acceleration reduces due to the rupture of the isolators. Moreover it should be noticed, although the ratio of the ruptured isolators at Pmax reaches from 20% to 30% to the total, these partial rupture phenomena do not necessarily cause the whole rupture.

The changes of the maximum response values in D-MCS are shown in Fig.10. As the input acceleration level increases, the maximum response displacement and velocity gradually increase, whereas the maximum response acceleration does not change. As for the maximum response velocity, there is no difference between the cases of COV equal to 0% and 20%.

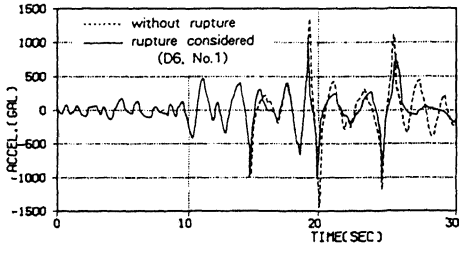

Fig. 8 Time history for the response acceleration.

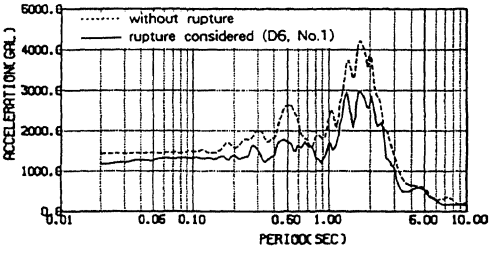

Fig. 9 Floor response spectrum for the acceleration.

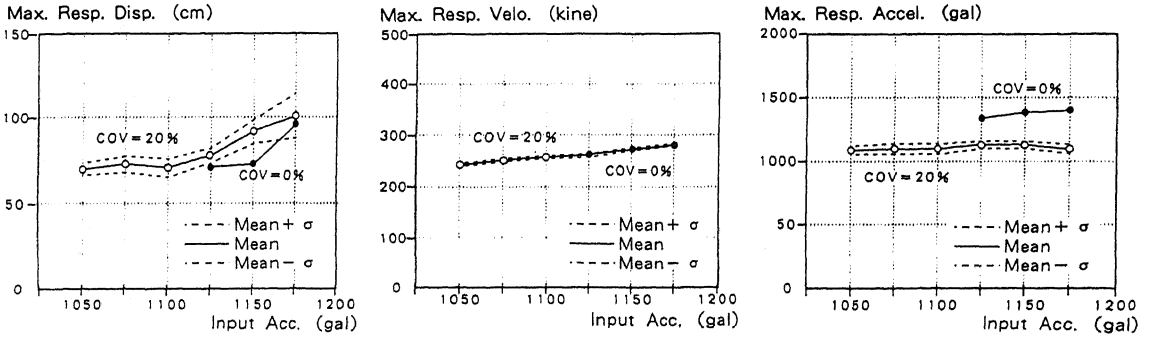

(a) Displacement. (b) Velocity. (c) Acceleration.

Fig.10 Changes of the maximum response value.

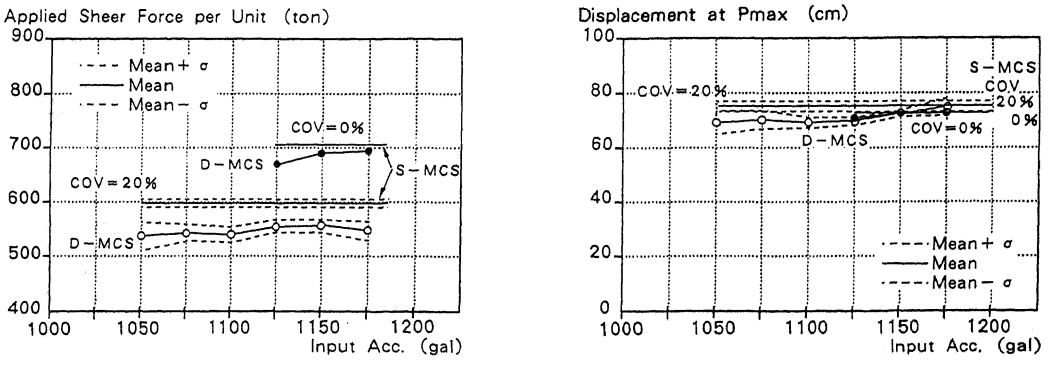

(a) Applied shear force per unit. (b) Displacement at Pmax.

Fig.11 Comparison of the results between S-MCS and D-MCS.

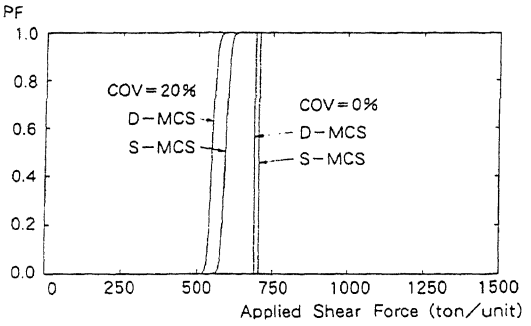

Fig.12 Comparison of the failure probability between S-MCS and D-MCS.

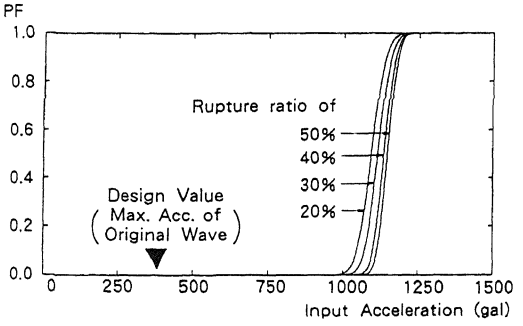

Fig.13 Comparison of the failure probability between rupture ratios based on D-MCS.

Fig.11 shows the comparison of the results between S-MCS and D-MCS. The average applied shear force per unit (=Pmax/272) for D-MCS is smaller than that for S-MCS, due to the influence on the reversal loadings. But in case of D6 (1,175gal) where the rupture ratio reached over 50% to the total, the horizontal displacement at Pmax nearly coincides with that in case of S1 for S-MCS.

Fig.12 and Fig.13 show the evaluated failure propability(fragility curve) of the seismic isolation system for the applied shear force and the input acceleration level, respectively. In these cases the criteria of the failure of the isolation layer are the same for S-MCS and D-MCS, i.e., when the horizontal load applied to the isolation layer exceeds the peak value, the failure is judged to occur. As shown in Fig.12, the tendency of the fragility curve based on D-MCS is the same as that based on S-MCS. The fragility curve derived from D-MCS nearly coincides with that from S-MCS in the case COV is equal to 0%, but the former one shifts to the lower side than the latter one in the case COV is equal to 20%. In Fig.13, there is a small difference in the fragility curve according to the rupture ratio which tentatively defines the dynamic failure of the isolation layer, but it is recognized that the seismic isolation system ensures a very large margin of safety against the design value.

4 CONCLUSION

The reliability analyses are performed based on the static and dynamic Monte Carlo Simulations considering the randomness of the rupture strength of the isolators in the seismic isolation layer. Qualitatively evaluated are the ultimate capacity of the seismic isolation layer, the influence on the behavior of the superstructure due to the rupture phenomena of the isolators, and the stability of the seismic isolation system. Conclusions are the following;

1)As the results of D-MCS, the elongation of the natural period occurs and the input energy to the superstructure is reduced due to the rupture phenomena. It is recognized that the partial rupture of the isolators does not immediately lead to the whole rupture because of "group effect" of the isolators as a parallel system.

2)There is some difference in the maximum response displacement and acceleration between the cases of COV equal to 0% and 20%, but no difference in the maximum response velocity.

3)As the results of S-MCS, the average applied shear force per unit device at the maximum strength becomes smaller, as the height of the mass and the COV of the rupture strength become respectively higher and greater.

4)There is some difference in the average applied shear force at the maximum shear strength between S-MCS and D-MCS, which is due to the influence of the reversal loadings. But there is no difference in the displacement to the maximum shear force between both MCS .

5)Failure probability is evaluated against the appilied shear force per unit and the input acceleration level. Failure probability evaluated from D-MCS becomes larger than that from S-MCS, when the applied shear force is small. However as a conclusing remarks, it should be emphasized that the seismic isolation layer ensures a large margin of safety againt the design earthquake motion.

Acknowledgements

This present research was sponsored by Ministory of International Trade and Industry in Japan.

Reference

[1] T. Mazda, M. Moteki, et al.:TEST ON LARGE-SCALE SEISMIC ISOLATION ELEMENTS, Trans. 11 SMiRT K25/4 pp.235-240,1991.